Impact of ZnO on the Physical and Optical Properties of $PbO–B_2O_3$ Glasses

J. Singh[a], G.P. Singh[a,*], P. Kaur[a], T. Singh[a], S. Bhatia[a], R. Kaur[b] and D.P. Singh[c]

[a] *P.G. Department of Physics, Khalsa College, Amritsar 143002, India*
[b] *P.G. Department of Physics, Lyallpur Khalsa College, Jalandhar 144001, India*
[c] *Department of Physics, Guru Nanak Dev University, Amritsar 143005, India*

Received: 24.12.2021 & Accepted: 06.06.2022

Doi: 10.12693/APhysPolA.142.195 *e-mail: gp_physics96@yahoo.co.in

The structure of the xZnO–30PbO–$(70-x)B_2O_3$ (x = 5–20 mol%) glass system is investigated by analysing the physical parameters like molar volume and density. An increase in density (5.31–5.7 g/cm^3) and consistent decrease in molar volume (20.95–20.03 cm^3/mol) of glass samples is observed with the rise in ZnO content. The X-ray diffraction pattern confirms the amorphous nature of glass samples. The ultraviolet-visible spectroscopy technique is utilized to detect changes in optical parameters, like optical band gap and refractive index. The results depicted a reduction in optical band gap (2.63–2.41 eV) with an increase in ZnO content. Other parameters, such as oxygen packing density, ionic behaviour and average boron-boron separation of prepared glasses, have also shown a variation with a change in ZnO content. Infrared Spectroscopy measurements confirm the change of borate coordination from trigonal BO_3 to tetrahedral BO_4.

topics: glasses, band gap, density, molar volume

1. Introduction

Glasses have always captivated mankind, fulfilling the needs of diverse technological areas due to their unique ability to be fabricated in a variety of compositions as required by the particular application [1–3]. Borate glasses have the highest glass forming tendency because they do not crystallize even at slow cooling rates. Apart from this, borate glasses also exhibit high transparency at lower temperatures [4]. Borate or B_2O_3 can develop glass with BO_3 units alone, however, when different cations are added, the BO_3 units are converted into BO_4 units. This is possibly due to the borate's high flexibility in creating the BO_4 tetrahedral structure rather than yielding non-bridged oxygen and rupturing B–O–B bridges [5].

In recent times, transition metal oxide (TMO) doped glasses have received a lot of attention because of their valuable physical, optical and electrical properties [6, 7]. Among transition metal oxides, Zinc oxide (ZnO) is the most suitable glass former as it is known to lower the viscosity at the melting temperatures of oxide glasses. In other words, it has a lower softening point compared to other types of glasses. This unique property of ZnO has a notable impact on the properties of the glasses. The impact of ZnO content on the structural properties of the glass is also very significant since it can play the role of the intermediate, i.e., it can behave as a network modifier as well as a network former depending upon the percentage composition [8–11]. Zinc oxide is a semiconducting material having a large band gap and is also regarded as a reliable material for visible and near-ultraviolet applications [12, 13]. It has numerous applications in the fabrication of electronic and optical devices, such as laser diodes, organic photovoltaics and light-emitting diodes (LEDs), due to its high dielectric constant and high exciton binding energy at room temperature [13–15]. Apart from that, ZnO is widely used as a radiation-resistant material, making it a suitable candidate for space applications [15, 16].

Borate glasses containing ZnO are expected to be highly electrically resistant, mechanically strong and thermal and chemically stable. In addition, these glasses are spectrally transparent in the visible and infrared ranges [17]. Extensive research is being pursued on transparent glass materials that are useful as insulating layers between the arrays of front electrodes in display panels. ZnO-based glasses meet all the prerequisites to be used for application in display panels [18, 19].

PbO glasses are commonly used in technological applications due to their unique properties, such as good radiation shielding [20], a large glass formation region, and low melting temperatures [21]. Borate

TABLE I

Composition, density, molar volume, and boron–boron separation (d_{B-B}) of the glass samples.

Glass	ZnO [%]	PbO [%]	B_2O_3 [%]	Density (D) [g/cm^3]	Molar volume (V_m) [cm^3/mol]	$\langle d_{B-B} \rangle$ [nm]
Zn-5	5	30	65	5.31	20.95	0.368
Zn-10	10	30	60	5.52	20.33	0.348
Zn-15	15	30	55	5.63	20.10	0.333
Zn-20	20	30	50	5.7	20.03	0.322

glass structures, in particular those containing lead, are significant due to their high light transmittance in the visible region of the electromagnetic spectrum [22]. Heavy metal oxides, such as PbO and ZnO, act as network exchangers in borate glasses, lowering their phonon energy [23].

The additive impact of zinc oxide (ZnO) on a glass system xZnO–30PbO–$(70-x)B_2O_3$ was investigated in this work, where x represents the different mole percentage of ZnO. The research aims to review the physical and optical properties of these glasses by examining X-ray diffraction patterns, density, molar volume, optical band gap, and other parameters to determine their compositional dependence on ZnO. This is necessary to determine the suitability of these glasses for a variety of applications.

2. Experimental details

The conventional melt-quenching technique is used for the preparation of glass samples of the type xZnO–30PbO–$(70-x)B_2O_3$ (x = 5–20 mol%), where x is the mole fraction of lead oxide (20–50%). The raw materials of zinc oxide (ZnO), lead oxide (PbO), and boric oxide (B_2O_3) in suitable quantities are mixed and ground finely to get a batch of 15 g. This mixture is then melted in a silica crucible in an electric furnace for one hour at a temperature of 1000°C in a normal atmosphere till a bubble-free liquid is formed. This bubble-free liquid is then quenched into a preheated steel mould and toughened at a temperature ranging from 400°C to room temperature to remove thermal and mechanical stress. Chemical data for all the above-mentioned glasses are shown in Table I.

2.1. Characterization

We have used the X-ray diffraction (XRD) technique to check the amorphous/crystalline nature of the samples using XRD-7000 (Shimadzu) X-ray diffractometer (Cu K_α, k = 1.54434 Å) at the rate of 2°/min and varied from 10 to 70° for 2 h. The density of glass samples is found using the standard Archimedes principle with the help of a sensitive microbalance, and pure benzene is used as the immersion fluid. The molar volume (V_m) is calculated using the formula

$$V_m = \frac{1}{D}\sum x_i M_i, \qquad (1)$$

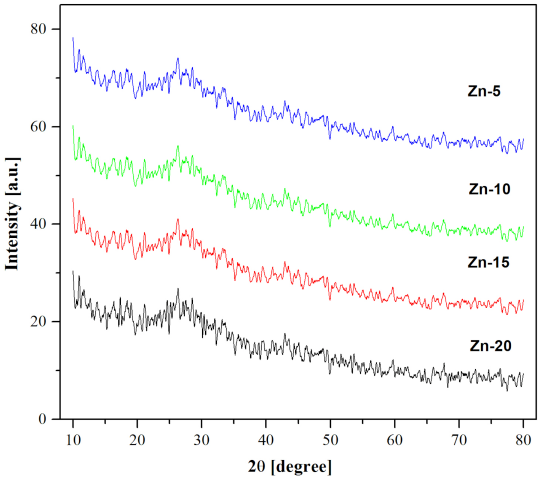

Fig. 1. X-Ray Diffraction of ZnO–PbO–B_2O_3 glasses.

where x_i is the molar fraction of the component and M_i is its molecular weight, and D is density. The optical absorption spectra of the polished samples were recorded with the help of a UV-Vis PerkinElmer Lambda 35 Spectrometer in the range of 200–800 nm at room temperature.

The infrared transmission spectra of the glasses were measured at room temperature in the wave number range 400–4000 cm^{-1} by a Fourier Transform computerized infrared spectrometer (Thermo Nicolet 380 spectrometer). The prepared glasses were mixed in the form of fine powder with KBr in the ratio of 1:100. The weighed mixtures were then subjected to a pressure of 150 kg/cm^2 to produce homogeneous pellets. The infrared transmission measurements were taken immediately after preparing the pellets.

Chemical data for all the above-mentioned glasses are shown in Table I.

3. Results and discussion

3.1. XRD spectral analysis

Figure 1 depicts the X-ray diffraction (XRD) pattern of prepared glass samples. The existence of broad humps and the absence of well-defined peaks confirms the amorphous nature of glasses [24].

3.2. Density and molar volume

Density is an important tool to detect the alteration in structure with changing glass composition. It has been discovered that the density of borate glasses shows a non-linear but increasing trend as ZnO is added at the expanse of B_2O_3. The fraction of four-coordinated borons or tetrahedral BO_4 units governs the density trend.

The density is determined using the following relation

$$\rho = \left(\frac{W_a}{W_a - W_b} \right) \rho_b. \tag{2}$$

In the present study of ZnO–PbO–B_2O_3 glasses, it has been observed that the value of density increases from 5.31 to 5.7 g/cm^3 with the addition of ZnO, as shown in Table I. This is due to the conversion of BO_3 units to BO_4 units as they contain more bridging oxygens, thus making the structure more compact. This trend continues with the further addition of ZnO. The inclusion of zinc is also thought to increase the density of glass due to the smaller ionic radius of Zn^{2+} compared to Pb^{2+} [$Pb^{2+}(1.32) > Zn^{2+}(0.74)$].

There is indeed a finite possibility that Zn^{2+} ions may be found at interstitial sites in the glass network. These factors (zinc ion size and formation of BO_4 groups) play a significant role in this hike in density.

The molar volume, which can be seen in Table I, shows the exactly reciprocal behaviour to that of density, as depicted in Fig. 2. This corresponding decrease in molar volume is caused by a reduction in bond length or interatomic spacing among glass network atoms which causes the structure to be compact.

3.3. Average boron–boron separation $\langle d_{B-B} \rangle$

Average boron–boron separation is calculated using the relation [25]

$$\langle d_{B-B} \rangle = \left[\frac{V_m}{2\,(1 - X_b) N_A} \right]^{1/3}, \tag{3}$$

where V_m is the molar volume, X_b is the molar fraction of B_2O_3, and N_A is Avogadro's number.

As the ZnO content increases, the value of $\langle d_{B-B} \rangle$ decreases continuously, and the presence of Zn^{2+} aids in the reduction of the average boron-boron separation. This alteration supports the role of ZnO as a modifier in the glass network. The addition of ZnO at low concentrations tends to result in the compaction of glass networks, which correlates well with the density and molar volume results, thus confirming them. The calculated $\langle d_{B-B} \rangle$ values are given in Table I.

3.4. UV-VIS absorption spectra

The UV-VIS absorption spectra of all the synthesised glasses have been investigated at room temperature. It can be seen that as the ZnO concentration increases, the band edge shifts to a higher wavelength, as shown in Fig. 3. The values of band edge wavelength observed from these graphs are displayed in Table II. This shift in band edge towards a longer wavelength is attributed to the availability of a large number of oxygen ions changing the glass network from trigonal (BO_3) to tetrahedral (BO_4) units [26].

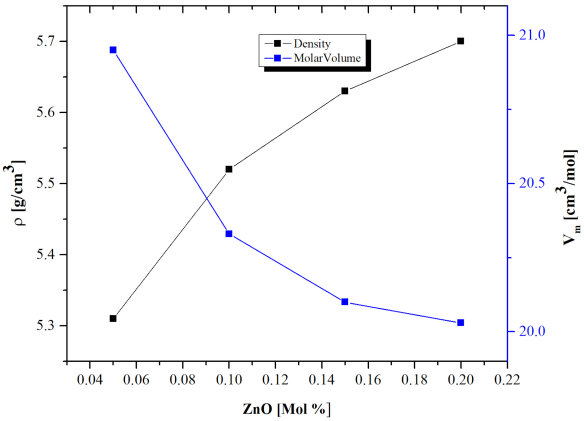

Fig. 2. Variation of density and molar volume for ZnO–PbO–B_2O_3 glasses.

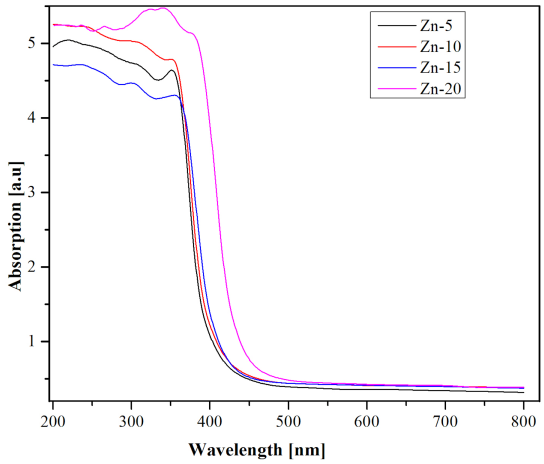

Fig. 3. Optical absorption of ZnO–PbO–B_2O_3 glasses.

UV-VIS absorption spectra have been used to evaluate the optical band gap by plotting Urbach graphs between $(\alpha h\nu)^{1/2}$ and energy $(h\nu)$ of ZnO–PbO–B_2O_3 glasses (Fig. 4). Here, α, h and ν and are the absorption coefficient, Planck's constant, and frequency, respectively. The plots indicate that the optical band gap in the glass samples decreases with the addition of ZnO, which again confirms the ZnO role as a network modifier. The preceding discussion demonstrates that the optical band gap energy is composition-dependent, so it can be adjusted by the varying composition of the material. This may help design some suitable semiconductor devices for special purpose solid state applications.

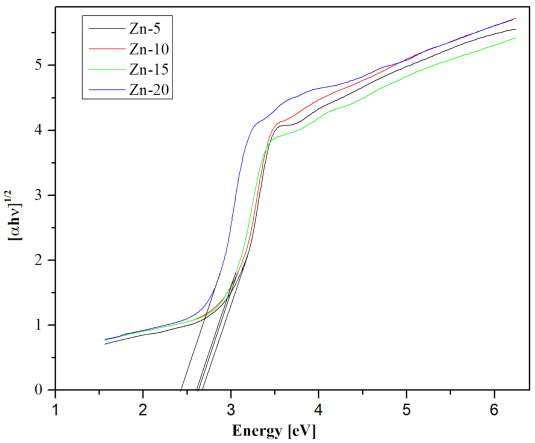

Fig. 4. Optical band gap of $ZnO–PbO–B_2O_3$ glasses.

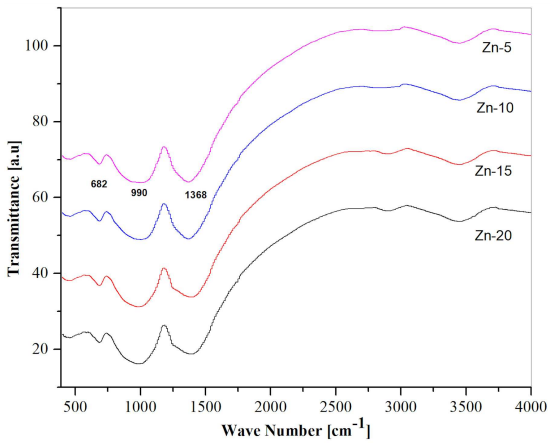

Fig. 5. FTIR of $ZnO–PbO–B_2O_3$ glasses.

TABLE II

Optical band gap, refractive index, oxygen packing density (OPD), covalency, and ionicity of the glass samples.

Glass	Optical band gap [eV]	Refractive index	OPD	Covalency	Ionicity
Zn-5	2.63	2.51	109.81	0.870	0.130
Zn-10	2.58	2.52	109.41	0.867	0.133
Zn-15	2.53	2.54	101.87	0.864	0.136
Zn-20	2.41	2.55	95.13	0.861	0.139

3.5. FTIR (Fourier transform infrared spectroscopy)

FTIR analysis is a powerful technique for investigating the essential structural unit arrangement and functional groups presented in the materials. The modes of vibrations of borate are investigated and classified into three IR regions [27].

In Fig. 5, the band in the range of 400–800 cm^{-1} occurs due to B–O–B bending vibrations of trigonal [BO_3] and tetrahedral [BO_4] group units [27, 28]. At 990 cm^{-1}, the band ranging from 800 to 1200 cm^{-1} is prevalent in sample Zn-5. This band is attributed to the stretching vibrations of the B–O bonds in BO_4 units of borate groups. At higher concentrations of ZnO, there is a slight shift of this band towards higher wavelengths along with an increase in its intensity [27, 28]. This observation provides strong evidence that as zinc levels rise, the BO_3 structural groups transform into tetrahedral BO_4 units, indicating that zinc acts as a modifier in the glass network. Furthermore, at 1368 cm^{-1}, broadband in the province of 1200–1600 cm^{-1} is observed, which is linked with the B–O stretching vibration of BO_3 units in various borate groups. The intensity of this band decreases as the ZnO content of the glasses increases [27, 28]. This shows that the presence of zinc oxide causes the conversion of BO_3 to BO_4 groups due to the availability of more oxygen.

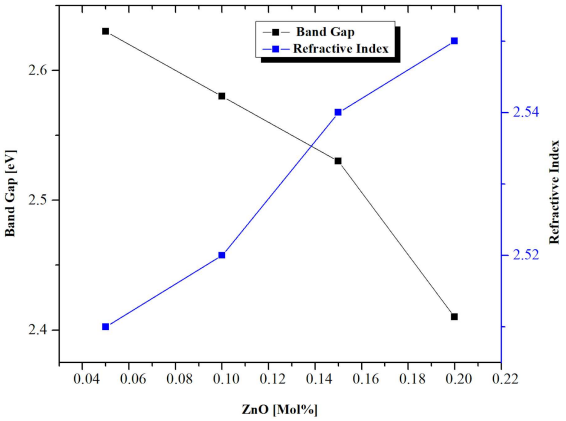

Fig. 6. Variation of optical band gap and refractive index for $ZnO–PbO–B_2O_3$ glasses.

3.6. Refractive index

The refractive index values also play a significant contribution to the material properties in various applications. It has been observed that the refractive index of glasses increases gradually with the decrease in optical band gap corresponding to thr increase in ZnO concentration. The calculated values are shown in Table II. The following factors are responsible for the increase in the refractive index:

- The change of the borate coordination from trigonal BO_3 to tetrahedral BO_4.
- The polarizability of Zn (0.286) being greater than that of B^{3+} (0.003).

The graph between refractive index, band gap, and mol% of ZnO shows the opposite trend as zinc concentration increases (Fig. 6).

3.7. Oxygen packing density

Oxygen packing density (OPD) is calculated from the density values using the following relation [28]

$$\mathrm{OPD} = 1000\, C\, \frac{\rho}{M} \tag{4}$$

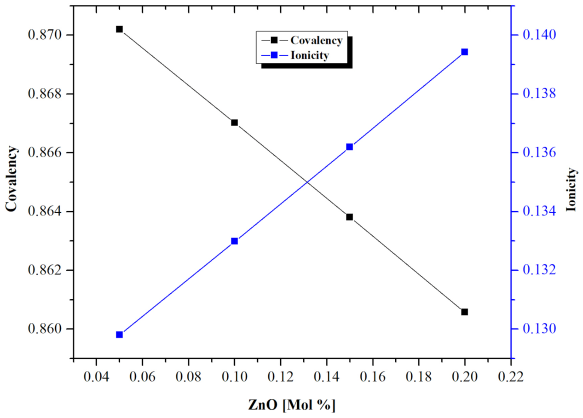

Fig. 7. Variation of ionicity and covalency for $ZnO–PbO–B_2O_3$ glasses.

where C is the number of oxygens per formula unit. Oxygen packing density decreases in accordance with the change in molar volume and density values. This is due to the formation of more bridging oxygens, which helps to create a compact glass structure, thus resulting in changes in the physical and chemical properties of the glass samples.

3.8. Covalency and ionicity

The covalency and ionicity of the glass samples are calculated using the relation given in the past study [29] and are shown in Table II. Figure 7 depicts the variation of ionicity and covalency for $ZnO–PbO–B_2O_3$ glasses with the percentage composition of ZnO. The trend indicates that covalency decreases and ionicity increases continuously with the rise in ZnO content in the glass samples. This behaviour confirms the transition of covalent bonds to ionic bonds inside the glass structure, which is responsible for a decrease in optical band gap with a rise in ZnO concentration.

4. Conclusions

In the present work, we successfully synthesized $ZnO–PbO–B_2O_3$ glasses with the help of a conventional melt quenching technique. Various calculated parameters like molar volume, density, refractive index, optical band gap, bond ionicity and covalency are in good agreement with one another.

X-ray diffraction study confirms amorphous structure of glass samples as no sharp peaks are observed. The density of glass samples increases with the increase in ZnO content and hence causes a corresponding reduction in molar volume, indicating the compaction of the glass network due to the formation of BO_4 units and smaller ionic radius of Zn^{2+} compared to Pb^{2+}. The optical band gap increases with an increase in zinc oxide content, confirming the role of ZnO as a network modifier in the glass networks. FTIR measurements confirm that the borate coordination is changed from trigonal BO_3 to tetrahedral BO_4. The refractive index increases gradually with the decrease in the optical band gap. Covalent behaviour decreases while ionic behaviour increases, indicating that the covalent bonds have been converted to ionic bonds.

References

[1] H.O. Tekin, S.A. Issa, E. Kavaz, E.A. Guclu, *Mater. Res. Express* **6**, 115212 (2019).

[2] Y.S. Rammah, H.M.H. Zakaly, S.A.M. Issa, H.O. Tekin, M.M. Hessien, H.A. Saudi, A.M.A. Henaish, *J. Mater. Sci. Mater. Electron.* **33**, 1877 (2022).

[3] Manjeet, A. Kumar, Anu, Ravina, Nisha Deopa, Anand Kumar, R.P. Chahal, S. Dahiya, R. Punia, A.S. Rao, *J. of Non-Crystal. Solids* **588**, 121613 (2022).

[4] J. Abhiram, R. Thejas, R.R. Ramakrishna, V. Pattar, A.R. Venugopal, K.M. Rajashekara, *AIP Conf. Proc.*. **2274**, 030034 (2020).

[5] S. Feller, in: *Springer Handbook of Glass*, Eds. J.D. Musgraves, J. Hu, L. Calvez, Springer Cham, 2019 p. 505.

[6] S. Hemalatha, M. Nagaraja, A. Madhu, K. Suresh, N. Srinatha, *Mater. Today Proc.* **49**, 1875 (2022).

[7] Z. Gao, S. Guo, X. Lu et al., *Adv. Opt. Mater.* **6**, 1701407 (2018).

[8] A.M. Al-Baradi, B.M. Alotaibi, N. Alharbi A.F. Abd El-Rehim, K.S. Shaaban, "Gamma Radiation Shielding and Mechanical Studies on Highly Dense Lithium Iron Borosilicate Glasses Modified by Zinc Oxide", *Silicon* (2022).

[9] Y. Al-Hadeethi, M.I. Sayyed, M. Nune, *Ceram. Int.* **47**, 3988 (2021).

[10] R. Stefan, E. Culea, P. Pascuta, *J. Non-Cryst. Solids* **358**, 839 (2012).

[11] Cetinkaya Colak, I. Akyuz, F. Atay, *J. Non-Cryst. Solids* **432**, 406 (2016).

[12] N. Sangwaranatee, P. Yasaka, R. Rajaramakrishna, S. Kothan, J. Kaewkhao, *J. Lumin.* **224**, 117275 (2020).

[13] L. Yuliantini, E. Kaewnuam, R. Hidayat, M. Djamal, K. Boonin, P. Yasaka, C. Wongdeeying, N. Kiwsakunkran, J. Kaewkhao, *Opt. Mater.* **85**, 382 (2018).

[14] N. Wu, Q. Luo, X. Qiao, C.Q. Ma, *Mater. Res. Express* **14**, 125901 (2015).

[15] Y.S. Rammah, FI El-Agwany, K.A. Mahmoud, A. Novatski, R. El-Mallawany, *J. Non-Cryst. Solids* **544**, 120162 (2020).

[16] Nada Alfryyan, Canel Eke, Zakaria M.M. Mahmoud, Z.A. Alrowaili, M.S. Al-Buriahi, *Rad. Phys. Chem.* **194**, 110044 (2022).

[17] D.N. Kim, J.Y. Lee, J.S. Huh, H.S. Kim, *J. Non-Cryst. Solids* **306**, 70 (2002).

[18] Qin Wang, Yao Tong, Meiting Yang, Hangtao Ye, Xiaojuan Liang, Xin Wang, Weidong Xiang, *J. Mater. Sci. Technol.* **121**, 140 (2022).

[19] J. Kaewkhao, K. Boonin, P. Yasaka, H.J. Kim, *Mater. Res. Bull.* **71**, 37 (2015).

[20] I. Kebaili, I. Boukhris, M.I. Sayyed, *Ceram. Int.* **46**, 19624 (2020).

[21] A. Górny, M. Kuwik, W.A. Pisarski, J. Pisarska, *Materials* **13**, 5022 (2020).

[22] A.S. Abouhaswa, Y.S. Rammah, S.E. Ibrahim, R. El-Mallawany, *J. Electron. Mater.* **48**, 5624 (2019).

[23] K. Swapna, S. Mahamuda, A.S. Rao, M. Jayasimhadri, S. Shakya, G.V. Prakash, *J. Lumin.* **156**, 180 (2014).

[24] H.M. Gomaa, H.A. Saudi, I.S. Yahia, H.Y. Zahran, *J. Mater. Sci. Mater. Electron.* **33**, 3284 (2022).

[25] A.M. Abdel-Aziz, R.A. Elsad, E.M. Ahmed, Y.S. Rammah, M.S. Shams, M.H. Misbah, *J. Mater. Sci. Mater. Electron.* **33**, 6603 (2022).

[26] J. Bhemarajam,P. Syam Prasad, M. Mohan Babu, M. Özcan, M. Prasad, *Compos. Sci.* **5**, 308 (2021).

[27] A. Aboalatta, J. Asad, M. Humaid, H. Musleh, S.K. Shaat, K. Ramadan, M.I. Sayyed, Y. Alajerami, N. Aldahoudi, *Nucl. Eng. Technol.* **53**, 3058 (2021).

[28] G.P. Singh, J. Singh, P. Kaur, T. Singh, R. Kaur, S. Kaur, D.P. Singh, *J. Alloys Compd.* **885**, 160939 (2021).

[29] M. Abdel-Baki, F.A. Abdel-Wahab, F. El-Diasty, *J. Appl. Phys.* **111**, 073506 (2012).